# Dimensionless Identity Experiments in JT-60U and JET

G Saibene[1], N Oyama[2], Y Andrew[3], JG Cordey[3], E de la Luna[4], C Giroud[3], K Guenther[3], T Hatae[2], GTA Huysmans[5], Y Kamada[2], MAH Kempenaars[6], A Loarte[1], J Lönnroth[7], D McDonald[3], A Meiggs[3], MFF Nave[8], V Parail[3], R Sartori[1], S Sharapov[3], J Stober[9], T Suzuki[2], M Takechi[2], K Toi[10], H Urano[2]

**1**. EFDA Close Support Unit - Garching 2 Boltzmannstrasse, 85748 Garching, Germany. **2**. Naka Fusion Research Establishment, JAERI, Ibaraki, Japan. **3.** Euratom/UKAEA Fusion Association, Culham Science Centre, Abingdon OX14 3EA, UK. **4**. CIEMAT-Euratom Association, Av Complutense 22, E28040 Madrid, Spain. **5.** Association Euratom/CEA, Cadarache, F13108 St. Paul-lez-Durance, France **6.** FOM-Rijnhuizen, Association Euratom-FOM, TEC, PO Box 1207, Nieuwegein, The Netherlands. **7**. Association Euratom-Tekes, Helsinki University of Technology, Finland. **8.** Centro de Fusao Nuclear, Euratom-IST Association, Av Rovisco Pais, Lisbon, Portugal. **9.** Association Euratom/IPP, MPI fur Plasmaphysik, 2 Boltzmannstrasse, Garching, Germany. **10**. National Institute for Fusion Science, Gifu, Japan

e-mail contact of main author: gabriella.saibene@efda.org

**Abstract.** This paper summarises results of dimensionless identity experiments in JT-60U and JET, aimed at the comparison of the H-mode pedestal and ELM behaviour in the two devices. Given their similar size, dimensionless matched plasmas are also similar in their dimensional parameters (in particular *a* is the same in JET and JT-60U). Power and density scans were carried out at two values of $I_p$, providing a q scan ($q_{95}$=3.1 and 5.1) with fixed (and matched) field. Contrary to expectations, a dimensionless match between the two devices was quite difficult to achieve. $p_{ped}$ in JT-60U is lower than in JET and, at low q, the pedestal pressure of JT-60U with a Type I ELMy edge is matched in JET only in the Type III ELM regime. At $q_{95}$=5.1, a dimensionless match in ρ*, ν* and $\beta_{p,ped}$ is obtained with Type I ELMs, but only with low-power JET H-modes. These results motivated a closer investigation of experimental conditions in the two devices, to identify possible "hidden" physics that prevents obtaining a good match of pedestal values over a large range of plasmas parameters. Ripple-induced fast ion losses of the large bore plasma used in JT-60U for the similarity experiments are identified as the main difference with JET. The magnitude of the JT-60U ripple losses is sufficient to induce counter-toroidal rotation in co-injected plasma. The influence of ripple losses was demonstrated at $q_{95}$=5.1: reducing ripple losses by ~2 (from 4.3 to 1.9MW) by replacing Positive with Negative Neutral Beam injection at ~ constant $P_{in}$, increased $p_{ped}$ in JT-60U, providing a good match to full power JET H-modes. At the same time, the counter-toroidal rotation decreased. Physics mechanisms relating ripple losses to pedestal performance are not yet identified, and the possible role of velocity shear in the pedestal MHD stability, as well as the possible influence of ripple on thermal ion transport are briefly discussed. Ripple losses in the ITER Q=10 reference scenario are negligible, and should not affect the plasma rotation. Although ITER plasmas will rotate at ~1/10 of the frequency of typical JET H-modes, results so far do not indicate that this should have a large effect on the pedestal MHD stability. On the other hand, the possible effect of ripple on thermal transport may deserve more attention, since the ripple magnitude of ITER is intermediate between that of JET and JT-60U.

## 1.Introduction.

This paper describes the results of dimensionless identity experiments in JT-60U and JET, aimed at the comparison of the plasma pedestal characteristics and ELM behaviour in the two devices. The method chosen for this study is the "dimensionless identity technique", based on the invariance of plasma physics to changes of dimensional parameters ($n_e$, $T_e$ at the pedestal, for instance), when the dimensionless plasma parameters are conserved (safety factor q, normalised plasma pressure β, Larmor radius ρ* and collisionality ν*). A simultaneous match of the four parameters above leads to the following scaling for the plasma current $I_p$, toroidal field $B_T$, density n and temperature T: $I_p \propto R^{-3/8}a^{1/8}$, $B_T \propto R^{5/8}a^{-15/8}$, $n \propto a^{-2}$ and $T \propto R^{5/4}a^{-7/4}$. In contrast to other dimensionless comparison experiments, the similar size of JET and JT-60U results in dimensionless matched plasmas that are also very similar in their dimensional parameters, with the exception of the major radius. The inverse aspect ratios ε differ, for the particular discharge geometry required by the experiments, by ≈15% ($\varepsilon_{JET}$ = 1.16 $\varepsilon_{JT\text{-}60U}$). The verification of dimensionless scalings in such highly constrained conditions (H-mode threshold power $P_{th}$, stored energy $W_p$, ELM frequency $f_{ELM}$, etc. should be very near in value) provides an excellent test-bed for the scaling hypothesis and for identifying any additional physics phenomenon that can affect extrapolations of present data to future devices.

## 2. The Experiment.

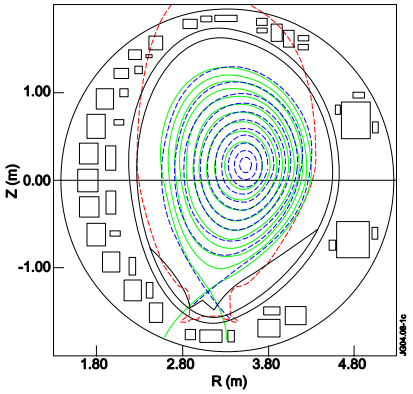


*FIG 1: poloidal cross-section of plasma equilibrium for pulse 41386 ($I_p$=1.8MA, $B_T$=3.1T) in JT-60U (green line) and in JET (blue, dashed line, pulse 59215, $I_p$=1.9MA, $B_T$=2.9T, shifted radially by +0.46m). The red dashed line represent the profile of the JET inner wall. .*

A special "JT-60U-like" equilibrium was developed in JET to match the magnetic geometry of the diagnostic optimised, large bore plasma used in JT-60U for H-mode pedestal studies (figure 1). This particular configuration in JT-60U, shifted to the low-field side of the device, suffers from relatively high ripple losses that limit the net available input power to the plasma. The plasma minor radius *a* is the same in the two devices, and geometric quantities such as elongation κ and triangularity δ are matched within ≤2% (κ~1.46, δ~0.27) [1].

The dimensionless identity comparison was focussed on 2 matching combinations of $I_p/B_T$: 1.8MA/3.1T (JT-60U) - 1.9MA/2.9T (JET), $q_{95}$=3.1 and 1.08MA/3.1T (JT-60U) - 1.15MA/2.9T (JET), $q_{95}$=5.1, providing a $q_{95}$ variation at constant $B_T$. The additional heating scheme in JT-60U was Positive Neutral Beam injection (PNB) or a combination of PNB and negative-ion neutral beam injection (NNB, at ~360kV, co-injection). In the JET experiments, most plasmas were PNB heated, while a few had PNB and ICRH hydrogen minority combined heating. While the injection energy of the PNB systems in JET and JT-60U is similar (80 and 110 keV in JET vs 85 keV in JT-60U), the injection geometry is not. Most of the PNB input power in JT-60U is provided by perpendicular injection (up to ~14MW), with further 4.4MW each available from co-injection and counter-injection sources. In the experiments described in this paper, the beam sources where always combined to provide net co-injection. In contrast, all the sources in JET are co-injecting, up to maximum input power of ~20MW. Input power and fuelling were varied to scan a range of edge densities and temperature, obtaining an overall variation of ν* at the pedestal between ~0.02 and 1, and of ρ* from ~2 $10^{-3}$ to 4.5 $10^{-3}$. The net input power $P_{in}$ was between 4-10MW (JET) and 6-10MW (JT-60U) at low current, while varied between 7 and 14MW (JET) and 10-13.5MW (JT-60U) at high current. The majority of discharges at both currents had a Type I ELM edge, but data in the Type III ELMy regime were also obtained, in both devices.

## 3. Results.

*3.1 Dimensional pedestal parameters*. The value of electron density ($n_{e,ped}$) and temperature ($T_{e,ped}$) at the top of the pedestal are compared in figures 2 and 3, for all discharges with $q_{95}$ of 3.1 and 5.1 respectively. The pedestal electron pressure ($p_{e,ped}$) of JT-60U plasmas tends to be lower than that of equivalent JET discharges, by up to a factor of two for PNB plasmas. In particular, for a given $n_{e,ped}$, the pedestal of JT-60U has lower temperature, both at low and high $I_p$. This is particularly evident for the higher $I_p$ experiments (figure 2), where the range of pedestal $n_e$-$T_e$ obtained in JT-60U with Type I ELMs is accessible in JET only if the plasma is deliberately driven to Type III ELMs. This is not the case for the low $I_p$, high $q_{95}$ experiments (figure 3): similar pedestal pressure for JET and JT-60U H-modes could be obtained by reducing the input power in JET (either PNB or PNB + ICRH) to levels near or below the empirical average minimum input power required to maintain a steady state Type I ELMy H-mode in JET (at this triangularity $(P_{in}/P_{th})_{min}$>2 [2], with $P_{th}$ from [3]). It is observed that at low power ($P_{in}/P_{th}$~1.8) and at low densities ($n/n_{GR}$<50%), compared to typical JET ELMy H-mode operation, Type I ELMy H-modes can be sustained although the pedestal is not "fully developed". In fact, in these conditions, $p_{ped}$ increases with $P_{in}$, although this dependence saturates at higher input powers. This "power dependence" of $p_{ped}$ is not observed for the JT-60U H-modes analysed in this paper, consistently with results from earlier analysis of low δ H-mode pedestals in JT-60U [4].

This behaviour of JET ELMy H-mode pedestals was successfully employed to "drive" the JET

pedestal parameters towards the values observed in JT-60U, resulting in the Type I ELMs points with $n_{e,ped}$~1.4 to 2.0 $10^{19}$and $T_{e,ped}$ between 0.8 and 1.3 keV, very near to typical Type I ELMy H-mode pedestal parameters of JT-60U similarity discharges. The marginality for Type I ELM pedestals in JET at these low input power is demonstrated by the co-existence at very similar pedestal parameters of Type I ELMy H-modes with plasmas at the transition between Type III and Type I regimes (black squares with a cross, fig. 3).

As mentioned in section 2, the large bore plasmas required in JT-60U for the identity experiments with JET suffer from large $B_T$ ripple-induced fast ion losses. In particular, the ripple perturbation at the low field side of the JET identity plasmas in JT-60 reaches 1.2%, to be compared with ~0.1% in JET. For the plasma configuration used in these experiments, the typical fast ion ripple losses are, for perpendicular injection, ~42% both at high and low $I_p$. Apart from limiting the total amount of net input power to the plasma, previous studies on JT-60U plasmas showed that ripple-induced ion losses can produce a counter-rotation source in the plasma edge [5,6]. This effect is quite prominent in the similarity plasmas studied here (figure 4): all plasmas with PNB injection rotate in the counter-current direction, in spite of positive (i.e. co-current) net momentum injection provided by the PNB. This is a clear difference with the JET experiments, where plasmas are always co-rotating for beam co-injection.

The possible effects of rotation and ripple losses on the pedestal were addressed experimentally in JT-60U, by reducing ripple-induced fast ion losses of the JET similarity plasmas by changing the beam make-up: most PNB perpendicular sources were substituted by NNB, reducing the power losses by ~50% (from ~4.3 to ~1.9 MW), and increasing the injected toroidal torque by a factor of ~2. The rotation at the plasma edge is reduced in magnitude, but does not change sign.

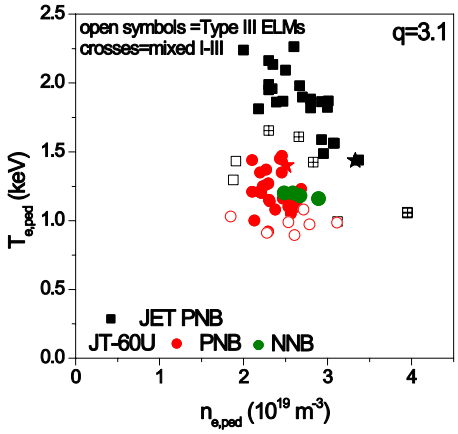


*FIG 2: comparison of JET and JT-60U pedestal $T_e$ vs. $n_e$ (top of the pedestal values), for all similarity discharges at $q_{95}$=3.1. The black squares are for JET data, the dots for JT-60U data: red with PNB injection and green with NNB injection. The stars highlight the dimensionless matching points.*

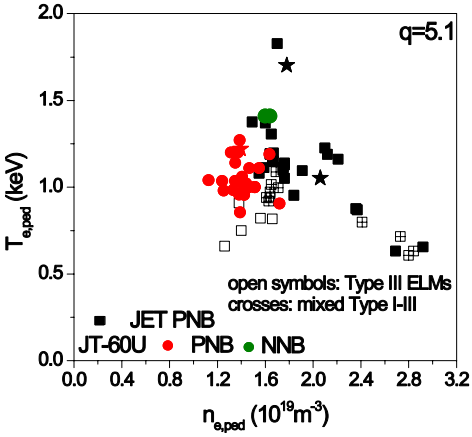


*FIG 3: $n_e$-$T_e$ diagram for the $q_{95}$=5.1 experiments, for both JET and JT-60U plasmas Same symbols as fig 2.*

At $q_{95}$, figure 3 (green dots) shows that NNB injection is correlated to a large increase in the pedestal parameters, achieving $p_{ped}$ above the maximum values obtained with PNB. In contrast, no clear improvement is observed at $q_{95}$=3, although the reduction in ripple-induced power losses and the changes in rotation at the plasma edge are similar for both currents.

*3.2 Dimensionless parameters analysis*. Figure 5 and 6 show the comparison of ρ*, ν* and $\beta_{p,ped}$ obtained in power/density scans at $q_{95}$=5.1 and $q_{95}$=3.1 respectively, including PNB and NNB heated plasmas in JT-60U and, for JET, PNB and PNB+ICRH H-modes. All the parameters are calculated at the pedestal top, with $\beta_{p,ped}$ defined as the total pedestal pressure normalised to the volume average poloidal field. Figure 5(a) shows that the range of $\rho_{tor}^*$ achieved in the two devices is similar, in particular if only Type I ELMy H-modes are considered. For $\rho_{tor}$*≤3 $10^{-3}$, JET and JT-60U pedestal (both PNB and NNB) have also similar ν*. For PNB discharges, a simultaneous match of $\rho_{tor}$*, ν* and $\beta_{p,ped}$ (q is fixed) between JET and JT-60U is found only for at relatively low pedestal pressures, for the JT-60U H-mode #45065 (@8.5s, $P_{in}$~8.8MW, $P_{in}/P_{th}$~2.5, with $P_{th}$ as reported in [7]), matching the JET low power ELMy H-mode #60849 (24s, $P_{in}$~7.6MW, $P_{in}/P_{th}$~1.8).

Figure 5 also shows that the high $\beta_{p,ped}$ H-modes in JET and JT-60U are obtained at completely different values of $\rho_{tor}$*. A somewhat different picture emerges if the pedestal data are cast in a dimensionless form using $\rho_{pol}$* instead of $\rho_{tor}$* (see figure 5(c), showing $\beta_{p,ped}$ as function of $\rho_{pol}$*). As highlighted in figure 5(c), a match is now obtained in the $\rho_{pol}$*-$\beta_{p,ped}$ space for the high $\beta_{p,ped}$ data obtained with NNB heating in JT-60U (example, #43075 @8.5s, $P_{in}$~9.4MW, $P_{in}/P_{th}$~2.7) and the JET ELMy H-mode at higher power (#60856, 21s, $P_{in}$~10MW, $P_{in}/P_{th}$~2.5). Interestingly, both JET and JT-60U report scaling of the H-mode pedestal width with $\rho_{pol}$ [8,9]. The corresponding ν* of the JET and JT-60U matching discharges are ~0.7 and 1.13 respectively. In this dimensionless pedestal parameters representation, JET and JT-60U PNB data now do not match very well, and the few points with comparable $\rho_{pol}$*-$\beta_{p,ped}$ have ν*differing by at least a factor of 3. The data points from the experiments at $q_{95}$=3.1 in the $\rho_{tor}$*-ν* and $\rho_{tor}$*-$\beta_{p,ped}$ spaces are shown in figure 6 (a) and (b). Both figures show that the common parameters space between the two devices is reduced compared to the high q case, in particular if one restricts the comparison to Type I ELMy H-modes only. Nonetheless, the JET #59219 (59s, $P_{in}$~11.2MW $P_{in}/P_{th}$~1.8, with gas fuelling to reduce $T_{ped}$, black star in the figures) is a good match to both JT-60U #43072 (6.4s, PBN, $P_{in}$~13MW, $P_{in}/P_{th}$~2.3) and #43059 (6.4s, NNB, $P_{in}$~12MW, $P_{in}/P_{th}$~2.8). The match between JET and JT-60U data is even poorer as function of $\rho_{pol}$*, in particular no match is found in terms of pedestal collisionality.

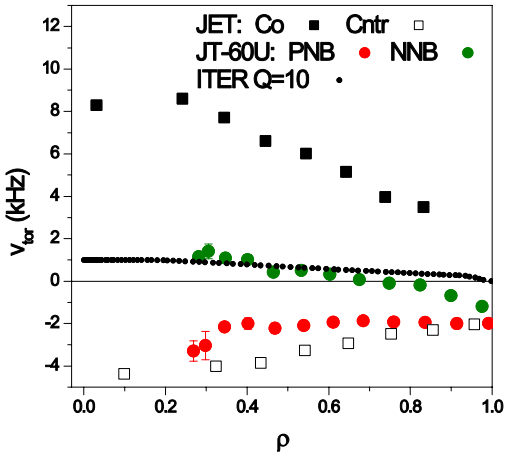


*FIG 4: typical toroidal rotation profiles (kHz) for JET and JT-60U plasmas. Black squares: # 59219 (1.8MA/2.9T) and, open black squares, # 59269 (for comparison, counter-injection, 2.5MA/2.4T not part of the similarity experiment). From JT-60U pulse 43075: red dots PNB only, green dots, NNB. Small black dots: expected $v_{tor}$ profile of the ITER Q=10 reference inductive scenario.*

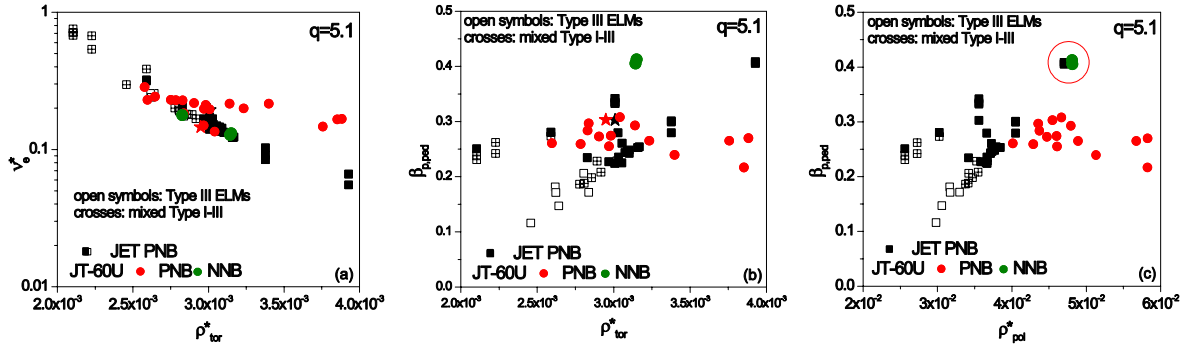


*FIG 5: dimensionless pedestal parameters for $q_{95}$=3.1 data in JET and JT-60U. (a) $\rho_{tor}$* vs ν*, (b) $\beta_{p,ped}$ vs $\rho_{tor}$* and (c) $\beta_{p,ped}$ vs $\rho_{pol}$*. Matching discharges with PNB heating are marked with a star.*

*3.3 Global confinement and ELM losses*. Although dimensionless identical H-mode pedestals have been obtained in JET and JT-60U, the global plasma confinement in JT-60U is systematically lower than in JET, also for matching pedestal conditions. This is illustrated in figure 7 for the $q_{95}$=5.1 dataset showing that the average $<H_{98}>$ of JT-60U type I ELMy H-mode is ~0.85 compared to ~1.1 for JET. At higher $I_p$, the picture is very similar, with $<H_{98}>$~0.75 for JT-60U, while in JET $<H_{98}>$~1.1. It is unlikely that this large difference in the confinement enhancement factor can be attributed to the small difference in the aspect ratio between the two devices (~15%). The core MHD activity is very similar in both JET and JT-60U, essentially dominated by sawteeth; discharges with NTMs have been excluded from this analysis. ELM frequency $f_{ELM}$ (as function of power crossing the separatrix, $P_{sep}$) and ELM power losses ($P_{ELM}$= $<\Delta W_{ELM}>\times f_{ELM}$, with $<\Delta W_{ELM}>$=average energy loss per ELM) have also been analysed for these experiments. Typically, for similar edge densities, $f_{ELM}$ is higher in JT-60U then in JET by a factor 1.5-3, for the same $P_{sep}$.

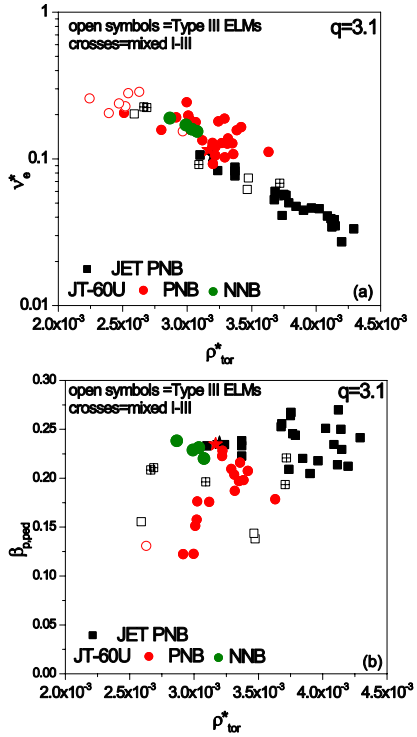


*FIG 6: dimensionless pedestal parameters for $q_{95}$=5.1 data in JET and JT-60U. (a) $\rho_{tor}$* vs $\nu$*, (b) $\beta_{p,ped}$ vs $\rho_{tor}$* Matching discharges with PNB heating are marked with a star*

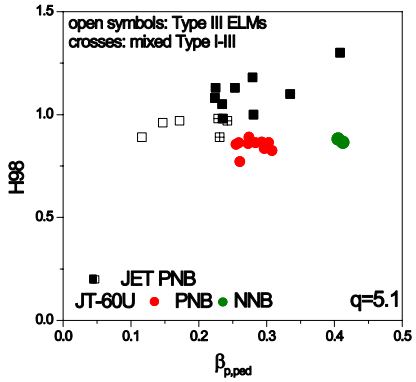


*FIG 7: $H_{98}$ as function of $\beta_{p,ped}$, for the $q_{95}$=5.1 dataset.*

The dimensionless ELM frequency ($f_{ELM}/\omega_{ce}$, with $\omega_{ce}$=eB/m) had been compared for the matching pairs of JET and JT-60U discharges. With the exception of the q=5.1 NNB JT-60U case, where $f_{ELM}/\omega_{ce}$ for the matched pair differ <10%, in all other cases the dimensionless frequencies do not match, with $f_{ELM}/\omega_{ce}$ (JT-60U) ~ 1.3-1.6 the JET values.

Finally, the fraction of power carried by Type I ELMs ($P_{ELM}/P_{sep}$) is very different in the two devices. For both currents, $P_{ELM}/P_{sep}$ in JT-60U ELMy H-modes is at most 20%, while in JET $P_{ELM}/P_{sep}$ is ~60%. This indicates that, for the same $P_{sep}$, the inter-ELM transport in JT-60U is much higher than in JET, since the plasma energy content of JT-60U is the same or lower than in JET.

*3.4 Plasma profiles comparison*. The comparison of the pedestal (and core) profiles of dimensionless matched JET and JT-60U H-modes may help to gain further insight in the underlying physics mechanisms determining the similarities and difference in the H-mode characteristics of the two devices. Figure 8 shows a comparison of some pedestal profiles for the matched discharges at $q_{95}$=5.1. Specifically, figure 8a compares the $T_e$ profiles for the pair #45065 (JT-60U, PNB) and JET #60849, while figure 8b shows the pedestal $n_e$ profiles for the same pair of shots. Figure 8c shows the $n_e$ profiles for the NNB JT-60U #43075, matching the JET pulse #60856. Figure 8a shows that, in matching conditions, a reasonable match is obtained for $T_e$ at the pedestal top. Pedestal widths and gradients are also comparable for both JET and JT-60U. More generally, a satisfactory agreement in value, width and gradients of $T_e$ is found for all dimensionless matched discharges, with PNB and NNB, and at both $q_{95}$.

The picture is quite different for the pedestal densities. The profiles compared in figure 8b are quite typical: the density pedestal of JET is much higher and wider than that of JT-60U, although the ratio between JET and JT-60U pedestal density height and width varies depending on the pair of discharges. A comparison of the edge density gradient $\nabla n_e$ is not straightforward for the discharges analysed here, since $n_e(r)$ of these JET discharges is measured with good space resolution only over a part of the pedestal density gradient region and the radial localisation of the FIR measurement is poor (~12cm).

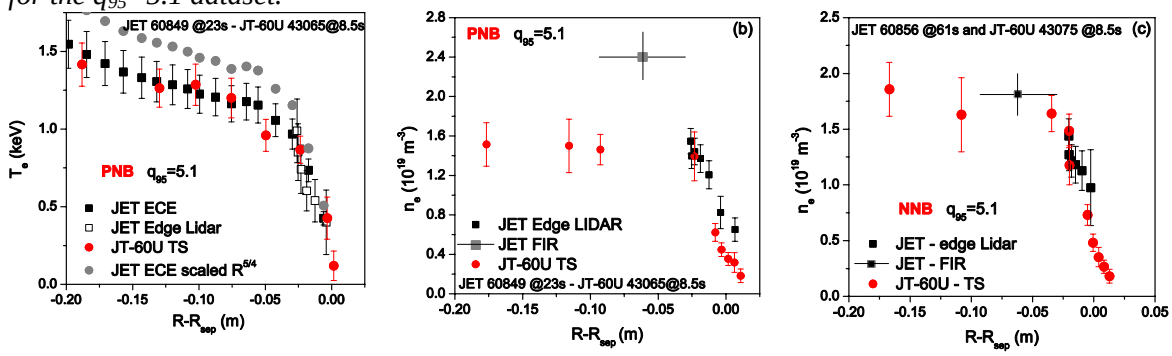


*FIG 8: pedestal profiles comparison for the two $q_{95}$=5.1 matched JET/JT-60U discharge pairs. 8(a): experimental $T_e$ profiles for #60849 (JET) and scaled values (grey dots); #43065(JT-60U, PNB) experimental values (red dots)). 8(b): density profiles for the same pair of pulses as 8(a). 8(c) $n_e$ profiles for #60856 (JET) and #43075 (JT-60U, NNB).*

Nonetheless, the indication is that, in general, the pedestal density profiles in JET are steeper than in JT-60U (see also [1]). The above considerations do not apply to the density of the $q_{95}$=5.1 JT-60U NNB heated discharge 43075 @8.5s (figure 8c): in this case the pedestal density obtained in JET and JT-60U are quite similar (within 15%), consistently with the improved pedestal pressure obtained with NNB heating in JT-60U H-modes at high $q_{95}$ (figure 3). Density gradients cannot be compared for the 2 pulses in figure 8c, because the JET edge Lidar settings were such that the measured gradient is limited by the instrument resolution. A more mixed picture emerges from the analysis of ion temperature data at the pedestal top (the edge $T_i$ profiles resolution for the JET pulses analysed here is not sufficient for a detailed profile comparison): at $q_{95}$=3.1, $T_{i,ped}$ (JT-60U)~$R^{5/4}T_{i,ped}$ (JET)~1.2 $T_{i,ped}$ (JET), as expected from the dimensionless scaling relations. This is not the case at $q_{95}$=5.1, where $T_i$ (JT-60U) is 20% lower than expected for the PNB case, and ~50% lower for the NNB discharge.

A comparison of the core profiles is quite complex, and would require a full transport analysis of the matching discharges, outside the scope of this paper. Nonetheless, some clear differences emerge from the inspection of the experimental profiles. First, all the JET discharges have standard H-mode core profiles, i.e. they do not have Internal Transport Barriers (ITB). This is not the case for the JT-60U pulses: most discharges (in particular at $q_{95}$=5.1) have an ITB, although the channel, strength and radial position of the ITB varied depending on the heating mix (PNB or NNB+PNB) and on $q_{95}$. For example, figure 9(a) shows a comparison of $T_i$ profiles for the matching discharges #59219 (JET, PNB) and JT-60U #43072 (PNB) and #43059 (NNB). A clear break in the slope of $T_i$ is visible for both PNB and NNB JT-60U pulses, absent in the JET profiles. In this example, the profiles outside the ITB radius have similar gradients in both devices. The density profiles for the same discharges are shown in figure 9b: these profiles show a distinctive feature that is common to many of the JT-60U plasmas analysed in this work: the profiles (in this case of $n_e$, but in other examples, also $T_e$ or $T_i$) have very flat gradients in the outer part of the plasma. Another example is shown in figure 9c, where $\nabla T_i$ of the JT-60U is much lower than for JET over the outer half of the plasma radius. The central $T_i$ values for the two discharges are similar because of the ITB on the ion channels for $\rho<0.5$. These observations point to differences in transport in the plasma core in the two devices, that clearly affect the plasma core energy content and could possible also influence the pedestal parameters. In the particular case of the $q_{95}$=3.1 discharges, the difference in the core density profiles is approximately sufficient to account for the lower stored energy compared to the JET case. As mentioned above, these empirical observations need to be substantiated by detailed transport analysis. This is left for future work.

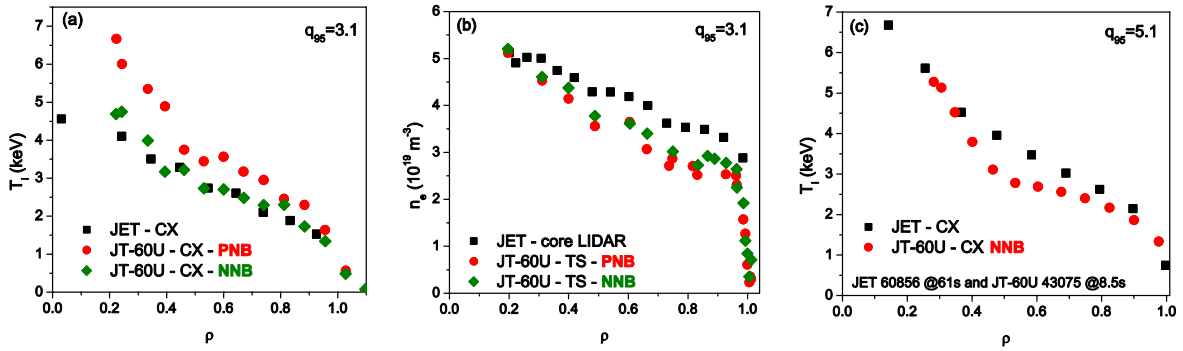


*FIG 9: comparison of JT-60U and JET core profiles, for a subset of the matched discharge pairs described in section 3.2. 9(a): $q_{95}$=3.1, $T_i$ profiles – JET data from core CX, JT-60U data from CX, one JET discharge #59219 selected as the match for both PNB and NNB JT-60U pulses. 9(b): density profiles for the same pulses as figure 9(a). 9(c): $q_{95}$=5.1 CX profiles of JET #60856 and JT-60U # 43075 @8.5s, NNB heating.*

## 4. Discussion

As described in section 1, the expectations from pedestal dimensionless identity experiments between JT-60U and JET was that the results would have provided a highly constrained but straightforward verification of the validity of the dimensionless scaling approach, given the very similar size of the two devices (resulting in dimensionless identical plasmas with very similar dimensional plasma

parameters). In reality, the experiments have shown the difficulty of obtaining correctly dimensionless scaled parameters in JET and JT-60U. The pedestal density and temperature of the JT-60U similarity H-mode reach, in general, values below those of JET (in real space): a dimensionless match of PNB heated H-modes in JT-60U and JET could be archived only by "downgrading" the H-mode pedestal performance of the JET similarity pulses, by operating at low power above the H-mode threshold and/or using external gas puff to reduce the pedestal pressure [2,8]

The discrepancy between experimental results and expectations motivated further comparative analysis of the experimental conditions on both devices, to identify other physics phenomena that may influence the pedestal characteristics. Two main differences are identified between JET and JT-60U identity plasmas: the inverse aspect ratio, and the magnitude of the $B_T$ ripple and fast ion losses.

The influence of ε (ε=0.29 for JET and 0.25 for JT-60U) on the pedestal MHD stability is discussed in detail in [1]. The influence of ε was evaluated starting from the ideal MHD analysis (carried out with the HELENA and MISHKA codes [10,11]) of Type I ELMy H-mode JET plasma, of the similarity series. The plasma and the walls where then moved rigidly outwards, changing ε in steps from the JET to the JT-60U value. It was found that the normalised pressure gradient $\alpha \propto \varepsilon$, and therefore the reduction in the sustainable pressure gradient (and of the total pressure, assuming similar pedestal widths) by aspect ratio effects is significantly less than observed experimentally.

A major difference between JET and JT-60U identity configuration is the $B_T$ ripple, ~0.1% in JET compared to ~1.2% in JT-60U (low field side – separatrix value). As mentioned in section 3.1, the associated fast ion losses in JT-60U are substantial, of the order of several MW for the plasma investigated, and the resulting edge electric field may provide a counter-rotation source at the plasma edge sufficient for JT-60U plasmas to counter-rotate even for net positive parallel momentum injection (figure 4). Experiments where a large fraction of perpendicular PNB were substituted by (low losses) co-NNB gave conflicting results: at low q, no significant increase of the pedestal pressure was observed, in contrast to the high q plasmas, were the use of NNB resulted in the highest pedestal pressures. In both cases, though, the plasma toroidal rotation changed in a similar way, consistently with the reduction of losses: $v_{tor}$ is less negative, as shown in figure 4 for the $q_{95}$=5.1 case. The reasons for the different behaviour of the pedestal pressure at low and high q, as well as that for the improved performance at high q are not yet understood.

Concentrating on the $q_{95}$=5.1 results, two possible mechanisms may be put forward to explain the improvement of the pedestal with reduced ripple losses.

The first is a possible effect of rotation on the pedestal ideal MHD stability. The pedestal MHD stability of the high $p_{ped}$ JT-60U #43075 @8.5s with NNB was analysed with the MISHKA-1 code and compared to that of the same discharge with PNB only (#43075 @5.5s). It is found that the experimentally calculated normalised pressure gradient in the s-α diagram ("operating point") reaches, at most, marginal access to second stability in the PNB phase of the discharge. In contrast, the high $p_{ped}$ obtained with NNB corresponds to the operating point entering the second stability region, with the normalised pressure gradient in the pedestal increasing as the edge magnetic shear decreases. For the same JT-60U discharge, the effect of plasma rotation (shear) was investigated with the MISHKA-D [12] code that includes finite gyro-radius effects of the ion diamagnetic drift on ideal MHD modes stability. It is found that, for the specific conditions analysed, imposing a negative toroidal velocity has a very small destabilising effects compared to the results from the MISHKA-1 analysis, insufficient to explain the large difference in pedestal pressures between the PNB and NNB phase of #43075.

A second idea under investigation is that ripple may have a direct effect on thermal ion transport. First results of simulations with the JETTO code, where ion transport is increased arbitrarily over different radial extents in the edge region of the plasma, seem to indicate that narrow layers (less than the pedestal width $\Delta_{ped}$) of enhanced transport may produce the reduction in pedestal and core performance. In particular, increasing the magnitude of the perturbation results in increasing ELM frequency and reduced maximum pedestal pressure. Assuming stiff temperature profiles, this results in an overall reduction of the plasma pressure. Interestingly, assuming a wide region of enhanced transport ($\sim 3\Delta_{ped}$) gives the opposite result: the increased losses reduce the ELM frequency, the average temperature at the pedestal increases, and so does the plasma global performance. The hypothesis of a direct effect of ripple losses on plasma transport has some further qualitative

resonance with some of the experimental findings reported earlier, in particular with the peculiar low-gradients of JT-60U density and/or temperature profiles in the outer part of the plasma (figure 9).

**5. Conclusions**

The results of these experiments, carried out between two fusion devices of very similar size, show that the dimensionless scaling approach for the prediction of plasma performance is valid only provided that no additional physics mechanism plays an important role. In the case of the JET/JT-60U, the large ripple losses in JT-60U are the most probable candidate causing the observed discrepancies between actual and scaled (predicted) pedestal plasma performances. The possible consequences for ITER may be different if the underlying physics mechanism is related either to effects of the magnitude and sign of velocity shear on the ideal MHD stability of the pedestal or to changes in plasma transport related to the magnitude and extent of the ripple perturbation.
The calculated $v_{tor}$ (ASTRA transport simulations) for the ITER Q=10 reference scenario is rather small but positive, as shown in figure 4. Since the predicted ripple losses in this ITER scenario are negligible, the expectation is that $v_{tor}$ will be positive. So far, the analysis of the experimental results indicates that the pedestal MHD stability is not strongly affected by rotation, even when it changes sign, therefore the expectation is that the small value of $v_{tor}$ in ITER should not affect the pedestal stability significantly. A detailed comparison of the MHD stability of plasma with varying edge velocity shear (experimentally determined) would allow a more quantitative evaluation of this effect.
The hypothesis of possible influence of toroidal field ripple on main plasma transport may have some relevance for the ITER plasma. For the Q=10 reference equilibrium, the value of the ripple at the separatrix at the outer midplane is ~0.6%, intermediate between JET and JT-60U. The present level of understanding of the effects of ripple on transport does not allow a prediction to be made for ITER at this point in time. An experimental investigation of the effects of $B_T$ ripple on H-mode pedestal and plasma performance is proposed for the coming experimental campaign of JET, in collaboration with JAERI. The experiments will taking advantage of the ability in JET of changing the ripple in a controlled way from ~0.1% to ~2% by controlling the differential current between odd and even TF coils, and therefore to reproduce both the JT-60U and ITER ripple values on the same device.

## Acknowledgements

The authors thank the EFDA-JET and JT-60U teams and collaborators for help and support in the execution and analysis of the joint experiments presented in this paper. On author (G Saibene) thanks Y Gribov and A Polevoi of the ITER IT-Naka for data on ITER ripple values and losses. Finally, these experiments have been carried out under the patronage of the ITPA, and in the framework of the IEA/LTA international agreement.

## References

[1] SAIBENE G et al., Plasma Phys Control Fus **46** (2004) A195-A205
[2] HORTON LD et al, Nucl Fusion **39** (1999) 993-1008
[3] ITER Physics Basis, Nucl Fusion **39** (1999) 2192-2198
[4] URANO H et al., Plasma Phys Control Fus, 44 (2002) A437-A443
[5] KOYDE Y et al., Plasma Phys Nuclear Control Fusion Res., **1** 777-789 IAEA CN-56/E-3-11
[6] TOBITA K et al., Nuclear Fusion **35** (1995), 1585-1591
[7] FUKUDA T et al., Plasma Phys Control Fusion **42** (200) A289-A297
[8] G SAIBENE et al., Nucl Fusion 39 (1999)
[9] KAMADA Y et al., 1996 Fusion Energy **1** 247 IAEA-CN-64/A1-6
[10] MIKHAILOWSKII AB et al., Plasma Phys Rep **23** (1997) 844
[11] LÖNNROTH J et al., Plasma Phys Control Fus 45 (2003) 1689
[12] HUYSMANS GTA et al., Phys. Plasmas **8** (2001) 4292